Universidade de Lisboa

Faculdade de Farmácia

Nystatin: Pioneering the Future of Antifungal Strategies in Combatting Infections

Joana Rita Gaspar Pereira

Trabalho de Campo orientado pela Professora Doutora Liana Silva,
Professora Auxiliar com Agregação

Mestrado Integrado em Ciências Farmacêuticas

2024

Universidade de Lisboa

Faculdade de Farmácia

Nystatin: Pioneering the Future of Antifungal Strategies in Combatting Infections

Joana Rita Gaspar Pereira

Trabalho Final de Mestrado Integrado em Ciências Farmacêuticas apresentado à Universidade de Lisboa através da Faculdade de Farmácia

Trabalho de Campo orientado pela Professora Doutora Liana Silva, Professora Auxiliar com Agregação

2024

Declaro ter desenvolvido e elaborado o presente trabalho em consonância com o Código de Conduta e de Boas Práticas da Universidade de Lisboa. Mais concretamente, afirmo não ter incorrido em qualquer das variedades de fraude académica, que aqui declaro conhecer, e que atendi à exigida referenciação de frases, extratos, imagens e outras formas de trabalho intelectual, assumindo na íntegra as responsabilidades da autoria.

Resumo

A interação entre a nistatina, um antifúngico de amplo espectro, e lipossomas, que são estruturas vesiculares formadas por fosfolípidos, pode ser um objeto de estudo muito relevante. A nistatina é um antifúngico de amplo espectro utilizado principalmente no tratamento de infeções cutâneas causadas por espécies de *Candida*. Embora eficaz, o seu uso terapêutico é limitado pela toxicidade sistémica e baixa permeabilidade intestinal. Deste modo, novas estratégias que permitam expandir o espectro de formulações de nistatina para tratar infeções fúngicas invasivas, abordando desafios como a toxicidade e a eficácia, são necessárias. Os lipossomas, compostos por bicamadas de fosfolipídios semelhantes às membranas biológicas, poderão constituir alternativas promissoras devido à sua biocompatibilidade, biodegradabilidade e capacidade de encapsular e direcionar fármacos de maneira específica. No entanto, para que estes sistemas de veiculação de fármacos sejam eficazes, é fundamental compreender as interações entre a Nys e os sistemas lipossomais, especialmente no que diz respeito a como a composição lipídica modula o mecanismo de ação da Nys e como este antifúngico afeta as propriedades das membranas e a integridade dos lipossomas.

A interação entre Nys e lipossomas foi avaliada principalmente por espectroscopia de fluorescência e espalhamento dinâmico de luz em diferentes misturas lipídicas. As misturas foram preparadas com POPC, EggSM e DPPC, compondo ambientes que simulam as propriedades estruturais e funcionais das membranas celulares. Os estudos de espectroscopia mostraram que em membranas contendo fase gel, a nistatina apresenta um desvio para o azul tanto no espectro de absorção como na emissão de fluorescência, acompanhado por um aumento da sua anisotropia, indicando uma maior rigidez e estabilização da nistatina na membrana.

No espalhamento dinâmico de luz, a dimensão das partículas de lipossomas demonstrou que houve uma variedade de populações, sugerindo uma possível agregação de vesículas, isto pode ser devido a uma instabilidade da membrana que poderia estar associada à formação de poros na membrana, especialmente em amostras de POPC/DPPC. Essas observações podem melhorar as perspetivas de tratamento para infeções sistémicas por fungos.

Palavras-chave: Biomembranas; Dispersão dinâmica de luz; Espectroscopia de fluorescência; Lipossomas; Nistatina

Abstract

The interaction between nystatin, a broad-spectrum antifungal, and liposomes, which are vesicular structures formed by phospholipids, could be a highly relevant subject of study. Nystatin is a broad-spectrum antifungal primarily used to treat skin infections caused by *Candida* species. Although effective, its therapeutic use is limited by systemic toxicity and low intestinal permeability. Thus, new strategies are needed to expand the range of nystatin formulations for treating invasive fungal infections, addressing challenges such as toxicity and efficacy. Liposomes, composed of phospholipid bilayers similar to biological membranes, may present promising alternatives due to their biocompatibility, biodegradability, and ability to encapsulate and specifically target drugs. However, for these drug delivery systems to be effective, it is essential to understand the interactions between Nys and liposomal systems, particularly regarding how lipid composition modulates Nys's mechanism of action and how this antifungal affects membrane properties and liposome integrity.

The interaction between Nys and liposomes was mainly assessed by fluorescence spectroscopy and dynamic light scattering in different lipid mixtures. These mixtures were prepared with POPC, EggSM, and DPPC, creating environments that simulate the structural and functional properties of cellular membranes. Spectroscopy studies showed that in membranes containing a gel phase, nystatin exhibited a blue shift in both its absorption and fluorescence emission spectra, accompanied by an increase in its anisotropy, indicating greater rigidity and stabilization of nystatin within the membrane.

In dynamic light scattering, the particle size of liposomes demonstrated a variety of populations, suggesting potential vesicle aggregation, which may be due to membrane instability that could be associated with pore formation in the membrane, especially in POPC/DPPC samples. These observations could improve treatment prospects for systemic fungal infections.

Keywords: Biomembranes; Dynamic light scattering; Fluorescence spectroscopy; Liposomes; Nystatin

Abbreviations

Abs	Absorbance
DDS	Drug Delivery Systems
DLS	Dynamic Light-scattering
DPPC	1,2 - Dipalmitoil-*sn*-glycero-3-phosphocholine
EggSM	Egg Sphingomyelin (ceramide-1-phosphorylcholine)
HEPES	4-(2-Hydroxyethyl)-1-piperazineethansulfonic acid
If_{max}	Maximum Fluorescence Intensity
LUV	Large Unilamellar Vesicles
MLV	Multilamellar Vesicles
Nys	Nystatin
PC	Phosphatidylcholine
PDI	Polydispersity Index
POPC	1-palmitoyl-2-oleoyl-*sn*-glycerol-3-phosphocholine
RI	Refractive Index
SUV	Small Unilamellar Vesicles
T_m	Main Phase Transition Temperature
***t*-PnA**	*trans*-parinaric Acid

Table of contents:

List of figures:

List of tables:

1 Introduction

1.1 Nystatin

While there have been significant advancements in developing antifungals for systemic mycoses, there's still a pressing need for more drugs that offer broad antifungal coverage, low toxicity, and affordability. (1)

Nystatin (Nys), an antifungal with membrane-active properties, is produced by *Streptomyces noursei* strains. It is available in multiple forms, including oral suspension, topical cream, and oral pastille. (2) Nys was the first polyene antifungal to be isolated and has a broad antifungal spectrum, making it an effective option for treating various fungal infections. It is active against nearly all pathogens listed in the "critical" and "high" priority groups of the WHO's list of priority pathogens. However, due to its systemic toxicity and low intestinal permeability, its therapeutic use is confined to treating cutaneous and mucocutaneous (vaginal and oral) fungal infections caused by *Candida* species. (3)

Nys (Figure 1) consists of three active components: nystatins A1, A2, and A3 (which are polyene macrolides featuring a diene-tetraene chromophore) and a flat macrolactone ring with a rigid polyene subunit containing conjugated double bonds, linked to a flexible polyosubunit with hydroxyl groups and a polar mycosamine head group. (3, 4)

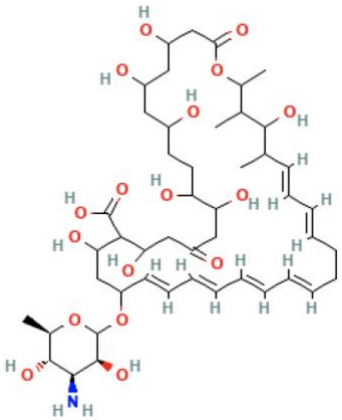

Figure 1. Chemical structure of nystatin

(PubChem)

The most accepted Nys action mechanism involves the creation of stoichiometric antifungal-sterol complexes that form barrel-like, membrane-spanning channels. (5) These channels compromise membrane function by allowing unregulated cation transport, ultimately resulting in cell death. The plasma membrane of organisms sensitive to antibiotics is the primary target of Nys and other polyene antifungal drugs. (6) In this mechanism of action Nys can permeabilize all types of sterol-containing vesicles, though the kinetics and structures formed differ: in cholesterol-containing vesicles, the initial pore formation rate is very slow, requiring higher amounts of nystatin to fully dissipate the K+ gradient and in ergosterol is able to induce the formation of highly fluorescent antibiotic aggregates alongside an immediate dissipation of the gradient. (7) A recent study in yeast *Saccharomyces cerevisiae* found a notable presence of highly ordered, sterol-free, gel-like sphingolipid microdomains in the plasma membrane under physiological conditions. This discovery suggests that polyene macrolides, such as nystatin, might exert their effects through a sterol-independent mechanism. (8) Thus, research aiming to unravel the specific antifungal-lipid interactions is fundamental as developing a systemic formulation of nystatin could expand antifungal drug options, improve efficacy, and reduce toxicity in treating invasive mycoses. The present study addresses this issue, by analyzing how Nys interacts with different lipids in the absence of sterols. To this end, membranes containing gel phase (DPPC), gel-fluid phase separation (POPC/DPPC 1:1) and fluid phase (POPC and POPC/EggSM 7:3) were selected to explore Nys interactions both with different lipids and membranes with different composition. The choice of EggSM is also relevant due to its status as the most abundant sphingolipid in mammalian cells, and, because of its properties, it can form extensive hydrogen bonds that may influence the interaction with Nys. Additionally, the role of ceramide within this sphingolipid further contributes to its potential interaction with Nys, making it a significant component in studies involving membrane-drug interactions. (9,10)

1.2 Liposomes

Liposomes, composed of self-assembling phospholipids forming lipid bilayers, are spherical vesicles enclosing an aqueous core. (11) They are extensively studied for their use in drug delivery and as models for biological membranes because they possess

multiple properties, due to their composition of lipids like those found in biological membranes, making them biodegradable, biocompatible, non-immunogenic, and non-toxic. (12) These molecules are amphiphilic, so they have hydrophilic heads and hydrophobic tails. In water, they form bilayer structures with the heads facing the water and the tails facing inward, creating liposomes. It's their amphiphilic properties that confer self-assembly, emulsifying, and wetting characteristics. Liposomal formulations often face stability issues - physical, chemical, and biological - related to both the membrane and the active substance, leading to degradation products and reduced therapeutic activity, and overall affecting their development and application. (13)

Liposomes can be categorized based on their size and the number of bilayers: multilamellar vesicles (MLV), large unilamellar vesicles (LUV), and small unilamellar vesicles (SUV). (14)

One of the methods used for the liposome formation is the film method. This method can be used to prepare all lipid vesicles: preparing lipids for hydration, hydrating with agitation, and sizing to get a uniform distribution of vesicles and in the end are produced heterogeneous multilamellar liposomes. While the film method is versatile and easy, scaling up is challenging and additional processing can increase time and costs. Downsizing techniques like sonication, homogenization, and extrusion are used to create more uniform vesicles. (15)

The use of liposomes as a drug delivery method has advantages as improving and controlling pharmacokinetics and pharmacodynamics, decreasing toxicity, enhancing drug activity against intracellular pathogens, target-selective liposomes, and enhancing activity against extracellular pathogens. (16) Also a larger fraction of the drug can be delivered to the diseased area minimizing its exposure to healthy tissues, using site-specific targeting and upon systemic administration, liposomes can recognize and bind to target cells with higher specificity. (17)

This study focuses solely on examining how Nys interacts with liposomes, laying the groundwork for future analyses in drug delivery research. Key parameters include drug interaction with the lipids (analyzed by fluorescence spectroscopy), and average particle size (z-average) and polydispersity index (PDI) (both analyzed by DLS). (18)

1.3 Membrane lipids

The biomembrane is a natural barrier that helps to separate the environment of cells and organelles, it not only provides structural integrity to cells but also regulate permeability allowing selective transport of molecules that is essential for maintaining homeostasis, among many other functions. This selective permeability enables cells to control their internal environment by balancing ions, nutrients, and waste products. (19) In its composition there are mainly lipids (phospholipids, glycolipids, and cholesterol, each with distinct properties that influence membrane structure and function), sterols, proteins. (20) Glycerophospholipids consist of two nonpolar hydrocarbon chains attached to a glycerol molecule, which is linked to a phosphate group. These phospholipids form the primary components of cell membranes, with phosphatidylcholine (PC) alone comprising 71% of all phospholipids in the human cell membrane. The lipid composition of membranes determines their fluidity by regulating the synthesis of fatty acids with varying chain lengths and degrees of unsaturation. (18)

A key characteristic of the lipids is their thermoreversible phase transitions, especially the "Main Phase Transition Temperature" (T_m), which plays a crucial role in determining the structure of biomembranes. Each lipid type has a specific T_m, that marks the shift from a gel ordered phase, characterized by a compact and orderly arrangement of acyl chains, to a more fluid, disordered liquid-crystalline structure as temperature rises. Thus, below T_m, the phase is solid-ordered, while above it, the phase becomes liquid-disordered. (21) Two different phospholipids were chosen because of their T_m differences: POPC - 1-palmitoyl-2-oleoyl-*sn*-glycero-3-phosphocholine - and DPPC - 1,2-dipalmitoyl-*sn*-glycero-3-phosphocholine (Figure 2). POPC and DPPC have a T_m of -2.9, +41.3 ºC, respectively, meaning that at room temperature, POPC exists in the liquid phase, while DPPC remains in the gel phase. (18,22) If lipidic mixtures of the two are made it means a liquid disordered and a gel phase may coexist.

a

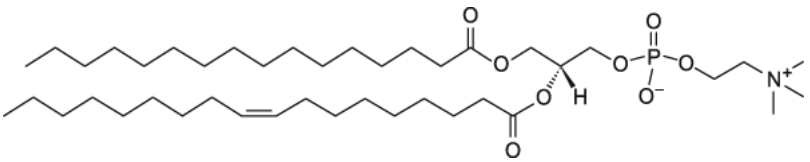

b

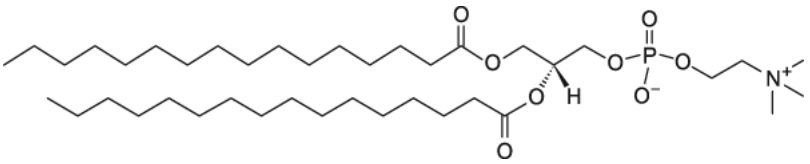

Figure 2. Chemical structure of POPC (a) and DPPC (b)

(Avanti)

Sphingomyelin (SM) (ceramide-1-phosphorylcholine) (Figure 3), is a sphingolipid, which consists of a ceramide with a phosphorylcholine head group. (23) EggSM has a T_m +38 ºC, presenting a gel phase at room temperature. (24) Ceramide derivatives are important in this work due to their unique characteristics: they organize fluid lipids and have a strong tendency to phase-separate. These properties play a role in membrane processes such as budding, fusion, blebbing, and other morphological changes. (10)

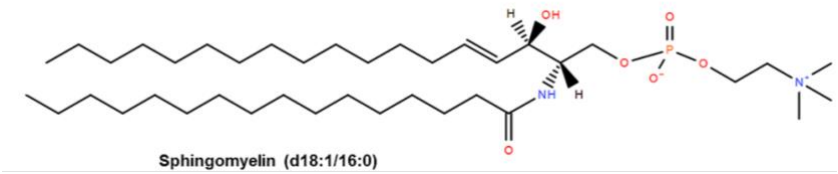

Figure 3. Chemical structure of SM (d18:1/16:0)

(23)

A study suggests that active Nys species formation is influenced by lipid type and the presence of ordered gel domains, affecting both Nys stability within the membrane and the degree of membrane permeabilization. Pore formation is more likely at gel/fluid boundaries, while in fluid membranes, permeabilization remains moderate. In a DPPC-enriched gel phase, Nys molecules were effectively incorporated and stabilized, leading to the formation of rigid, active pores. Conversely, in an SM-enriched gel phase, Nys disrupted the tightly packed structure by interfering with the hydrogen bonds among

sphingolipids. Active Nys species in this environment only formed when enough Nys molecules were present to destabilize the SM-enriched gel structure. (5)

1.4 Fluorescence spectroscopy

Fluorescence imaging can show where and how much of intracellular molecules there are, sometimes even detecting single molecules. It has a variety of applications in the pharmaceutical field, such as providing information on nanoparticles, the local environment of the drug, and details about the loaded drug molecules. Fluorescence spectral data are usually displayed as emission and excitation spectra, which plot fluorescence intensity against wavelength (nm) or wavenumber (cm^{-1}). These spectra can vary greatly based on the fluorophore's chemical structure and the solvent used. (17, 22)

Fluorescence happens when a molecule absorbs light at one wavelength and almost instantly re-emits it at a different, usually longer, wavelength. Both fluorescence and phosphorescence involve photon emission as molecules return from an excited state to a relaxed state. These processes include transitions between electronic and vibrational states of fluorescent molecules called fluorophores. (26)

The Jablonski diagram is commonly used to illustrate the sequence of processes that occur between light absorption and emission. Analyzing this diagram (Figure 4) reveals that emission energy is generally lower than absorption energy, meaning fluorescence tends to occur at longer wavelengths. A notable feature of fluorescence is that its emission spectrum remains consistent regardless of the excitation wavelength. The excitation and emission bands of a fluorophore are often the mirror image of each other. This symmetry in fluorescence spectra arises because the same electronic transitions and similar vibrational energy levels in the ground (S_0) and excited (S_1) states are involved in both absorption and emission. While this "mirror-image" relationship is often observed, there are many exceptions. In cases where the absorption spectrum of a fluorophore shows distinct peaks, these peaks correspond to transitions from the lowest vibrational level of the S_0 state to various vibrational levels of the S_1 state.

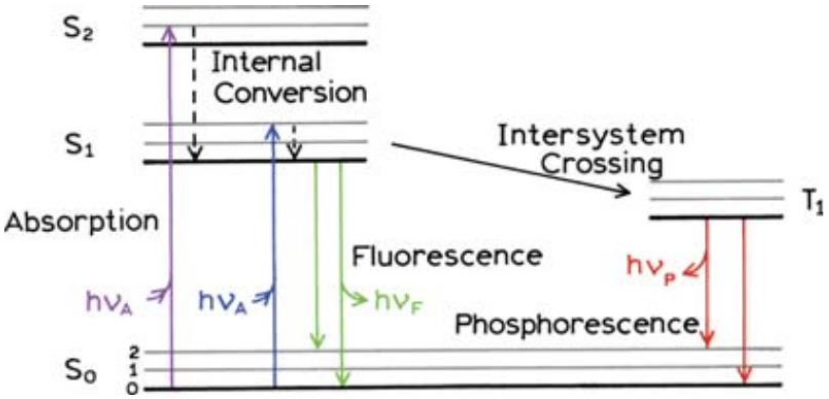

Figure 4. Jablonski diagram. Diagram illustrating the electronic states and photophysical processes of a molecule including the ground state (S_0), excited singlet states (S_1, S_2), and the triplet state (T_1) upward solid arrows represent the absorption of photons leading to electronic excitation downward solid arrows indicate radiative transitions such as fluorescence (S_1 to S_0) and phosphorescence (T_1 to S_0) dashed arrows represent non-radiative processes including internal conversion (between singlet states) and intersystem crossing (from a singlet to a triplet state).

(25)

Anisotropy measurements provide insights into the rigidity and fluidity of molecular environments, such as cell membranes, by revealing information about the surroundings of a fluorophore. These measurements rely on photoselective excitation, where polarized light selectively excites fluorophores aligned with its electric vector. In an isotropic solution, fluorophores are randomly oriented, but polarized light creates a partially oriented population, leading to partially polarized fluorescence emission. Anisotropy values reflect the fluorophore's rotational freedom: they are high in rigid environments and low in fluid ones, indicating sensitivity to the surrounding environment's dynamics. (25)

Rigid membrane environments have been studied in relation to Nys interactions with lipid membranes. In POPC/DPPC lipidic mixtures, an increase of fluorescence lifetime values, indicated an increase in molecular rigidity. Later this study showed that the kinetics and extent of Nys pore formation occur via different mechanisms that depend on lipid composition and the presence of gel–fluid phase separation, such as POPC/DPPC. This increased rigidity in the membrane may therefore play a key role in facilitating Nys-induced pore formation. (5,9)

1.4.1 *Trans*-parinaric acid and Nystatin

Trans-parinaric acid (*t*-PnA) is a fluorescent 18-carbon tetraene used to investigate the structure and dynamics of lipid bilayers, biological membranes, and lipophilic proteins. Its spectroscopic properties can be compared to those of nystatin, as both contain a conjugated tetraene chromophore. (24, 25) Polyene fluorophores, like *t*-PnA, and Nys have their chromophore embedded within the hydrophobic core or in the bilayer membrane surface of the lipid bilayer, enabling them to provide direct insights into the acyl chain packing. These fluorophores exhibit a strongly allowed electronic transition, which ensures efficient light absorption. However, their fluorescence emission originates from a weak lowest-energy transition. (29) Nys has intrinsic fluorescence being easily distinguished via their absorption spectra, because the tetraene typically shows vibronic absorption peaks at 292, 305, and 320 nm. (28)

Spectroscopic analysis enables the evaluation of the photophysical properties of the molecules under study, where shifts in wavelength and changes in emission and absorption intensities allow for a detailed examination of the molecular environment and the interactions they engage in. (10,30)

1.5 Dynamic light-scattering

Dynamic light-scattering (DLS) techniques are commonly used to measure the particle size distribution of materials in suspensions smaller than 1 μm. DLS offers a quick and straightforward method to detect particle size in suspension, relying on Brownian motion. (31) This technique is non-invasive, requires minimal sample preparation and no pre-experimental calibration and because of that has become a popular tool within pharmacy community. (32)

In this technique, a colloid dispersion is hit by a laser, scattering the light. The scattered light's intensity fluctuates over time due to the movement of particles causing constructive and destructive interferences. The intensity fluctuations are analyzed over time in a histogram, which allows for the observation that smaller particles move at higher speeds. As a result, the amplitude and width of the fluctuations provide valuable information regarding the distribution of particle sizes and the homogeneity of the sample. (33) Two important parameters measured in DLS are average particle size and PDI. PDI ranges from 0 to 1, where in theory, a value of zero represents a monodisperse

system. The PDI value of 0.1 to 0.7 represents nearly monodisperse preparation, whereas PDI > 0.7 suggests broad distribution of macromolecular sizes. (34)

The DLS results are influenced by several factors, such as the solvent's viscosity, the instrument used, sample concentration, temperature, and the material's refractive index or impurities. (35)

2 Aim of the Project

This study aims to investigate the effects of Nys on membranes of various lipid compositions to provide further insight into its mechanism of action (pore formation). Specifically, it seeks to support the hypothesis that nystatin can interact with sterol-free membranes containing gel-phase forming lipids. Understanding these interactions is essential for developing a systemic formulation of nystatin, which is currently available only in oral suspension, topical, and tablet forms. Utilizing liposomes as drug delivery systems (DDS) could enhance the therapeutic potential of nystatin.

3 Materials and Methods

3.1 Materials

POPC, DPPC and EggSM were purchased from Lipoid. All the lipids used were 99% pure reagents. Nys (CAS: 1400-61-9) and *t*-PnA were stored at -20°C in the dark. The concentration of Nys in stock solutions was determined spectroscopically, using a molar absorption coefficient of $\varepsilon = 6.3 \times 10^4\ M^{-1}\ cm^{-1}$ in ethanol at 304 nm and *t*-PnA a molar absorption coefficient of $\varepsilon = 8.9 \times 10^4\ M^{-1}\ cm^{-1}$ at 300 nm in ethanol. The other reagents and solvents used were of analytical grade.

3.2 Methods

3.2.1 Lipid Quantification

Quantification of the stock solution in the sample were measured via the Rouser method. First, a fixed volume of Na_2HPO_4 (0.5 mM) was added to glass vials in triplicate for a calibration curve, dried at 170°C in a Techne Dri-Block DB-3A thermoblock. The sample followed the same process with an appropriate volume. Next, 300 µL of perchloric acid was added to hydrolyze phospholipids, releasing inorganic phosphorus, and the mixture dried again at 170°C for 45 minutes. Once cooled to room temperature, 1 mL of water, 400 µL of ammonium molybdate (1.25%), and 400 µL of ascorbic acid (5%) were added sequentially. The mixture was stirred, heated in a water bath at 100°C for 5 minutes, and absorbance measured at 797 nm using a *Shimadzu UV-mini 1900* spectrophotometer. Samples were diluted as needed to ensure phosphate concentration was within the calibration curve limits.

3.2.2 Liposome preparation

In this experimental work four distinct liposomal formulations: POPC, POPC/DPPC at molar ratio 5:5, POPC/EggSM at molar ratio 7:3, DPPC were made from the known concentration stock solutions.

The liposomes were prepared in different ways to determine the best method. The goal was to assess the necessity of using a vacuum desiccator and nitrogen flow for drying

the samples. Three different procedures were carried out, and the lipid formulation used in each was as follows in table 1.

Table 1. Diagram of the different lipid composition and their molar ratio with the different procedures used.

Lipid Composition	Molar Ratio	With Desiccator and Nitrogen	Without Desiccator and with Nitrogen	Without Desiccator and without Nitrogen
POPC	-	1a	2a	3a
POPC/DPPC	5:5	1b	2b	3b
POPC/EggSM	7:3	1c	2c	-
DPPC	-	1d	2d	-

Lipid suspensions were prepared in the desired molar ratios as solutions in chloroform. The solvent was removed either by by nitrogen flow (methods 1 and 2), or by heating in the thermoblock Techne, Dri-block DB-3A at 90ºC for 15 minutes (method 3). In method (1) the lipid residue was further placed in the vacuum desiccator for 3 hours prior to hydration. The residual lipid films, warmed to 50°C in a water bath, were hydrated with HEPES buffer (HEPES 10mM; NaCl 150mM; pH 7.42) and repeatedly vortexed until all lipid was removed from the walls of the round-bottom flask. Then a freeze-thaw cycle was repeated eight times using and ice bath and a water bath warmed to 50°C. Subsequently, the lipid suspension was extruded 21 times through polycarbonate membranes of 100 nm pore size. LUV were prepared using the extrusion technique with the Avanti Mini Extruder at 50ºC.

3.2.3 Fluorescence analyzes

These measurements were conducted using a *Jasco FP-8550* Spectrofluorimeter. Both the samples and the fluorimeter were thermostated at 25°C. Steady-state fluorescence measurements were conducted at fixed excitation wavelengths of 320 nm for *t*-PnA and 303 nm for Nys, with emission wavelengths at 420 nm for *t*-PnA and 404 nm for Nys. The probe-to-lipid ratio used for *t*-PnA was 1/200 with a final added concentration of

1,93 μM of t-PnA. Nys concentrations of 5, 10, 15 μM were added in different samples. The measurements were performed using 1 cm x 0.4 cm quartz cells from *Helma Analytic*, with the longest optical path oriented along the excitation axis. Typically, excitation and emission slits of 4 nm were used. The steady-state anisotropies, $< r >$, were determined according to (25):

$$< r > = \frac{I_{VV} - GI_{VH}}{I_{VV} + 2GI_{VH}} \qquad (1)$$

where I_{ij} are the steady-state vertical and horizontal components of the fluorescence emission with excitation vertical (I_{VV} and I_{VH}) and horizontal (I_{VH} and I_{HH}) to the emission axis. Polarization measurements were made using Glan-Thompson prism polarizers in a single-channel detection system and an adequate blank was subtracted from each intensity reading before calculating the anisotropy value.

3.2.4 DLS analyzes

POPC and DPPC liposomes with a total lipid concentration of 1mM were diluted with HEPES buffer to a final concentration of 0.2mM. This dilution was performed to mitigate high turbidity, which could skew the results. The dispersant RI was set to 1.72, with a viscosity of 1.00 cP and the temperature of 25 ºC. DLS measurements were performed before (time 0) and 5, 30, 60 and 120 minutes after addition of 15μM of nystatin to the liposomes, using a *Malvern Nanoseries*. Control experiments were made with methanol in the different times and concentrations used.

The average particle diameter and PDI were determined from the mean of three measurements using the Zetasizer software.

4 Results

4.1 Characterization of lipid mixtures: effect of diverse preparation methods

4.1.1 Determination of the concentration of lipid stock solutions

The concentration of lipid stock solutions was determined using the Rouser method, a colorimetric assay that quantifies lipid phosphate content, allowing for accurate measurement of phospholipid concentrations. The experimental data obtained (Figure 5) enabled the calculation of concentrations for the various lipid solutions, as summarized in table 2. This precise determination was essential for maintaining the desired molar ratios in the lipid mixtures used throughout the experiments. The regression equation is as follows:

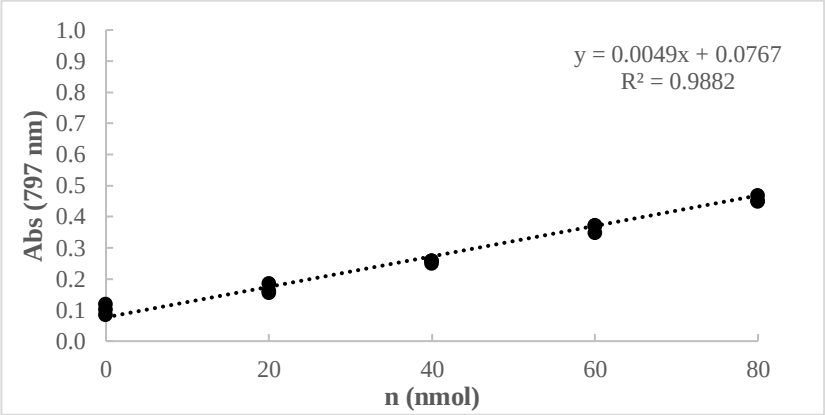

Figure 5. Calibration curve for phospholipid quantification using the Rouser method. The dotted line represents the linear fit across three replicates for each phosphate (Pi) amount.

Table 2. Stock solution concentration and absorbance of each lipid

Sample	Average Abs	Concentration (M)
POPC	0.460	1.58×10^{-2}
EggSM	0.409	1.36×10^{-2}
DPPC	0.266	1.29×10^{-2}

4.1.2 Characterization of lipid mixtures: Fluorescence analysis

Various methods were employed to search for the best way to obtaining the lipid film and remove the solvent. Therefore, a characterization with *t*-PnA was conducted to investigate potential significant changes in the properties of the liposomes prepared by the different methods 1, 2 and 3.

The spectral analysis of *t*-PnA in the lipid mixtures showed no significant differences across the different preparation methods, regardless of lipid composition, as showed in figure 6. This similarity in spectra suggests that the preparation technique, whether using or not the desiccator and nitrogen, did not alter the fluorescence characteristics of *t*-PnA in the various lipid environments tested. These results suggest that these minor modifications in the protocol do not have a significant impact on liposomes formation and properties. Therefore, we selected method 3 for further experiments, as it is faster and does not require nitrogen, simplifying the preparation process without compromising sample quality.

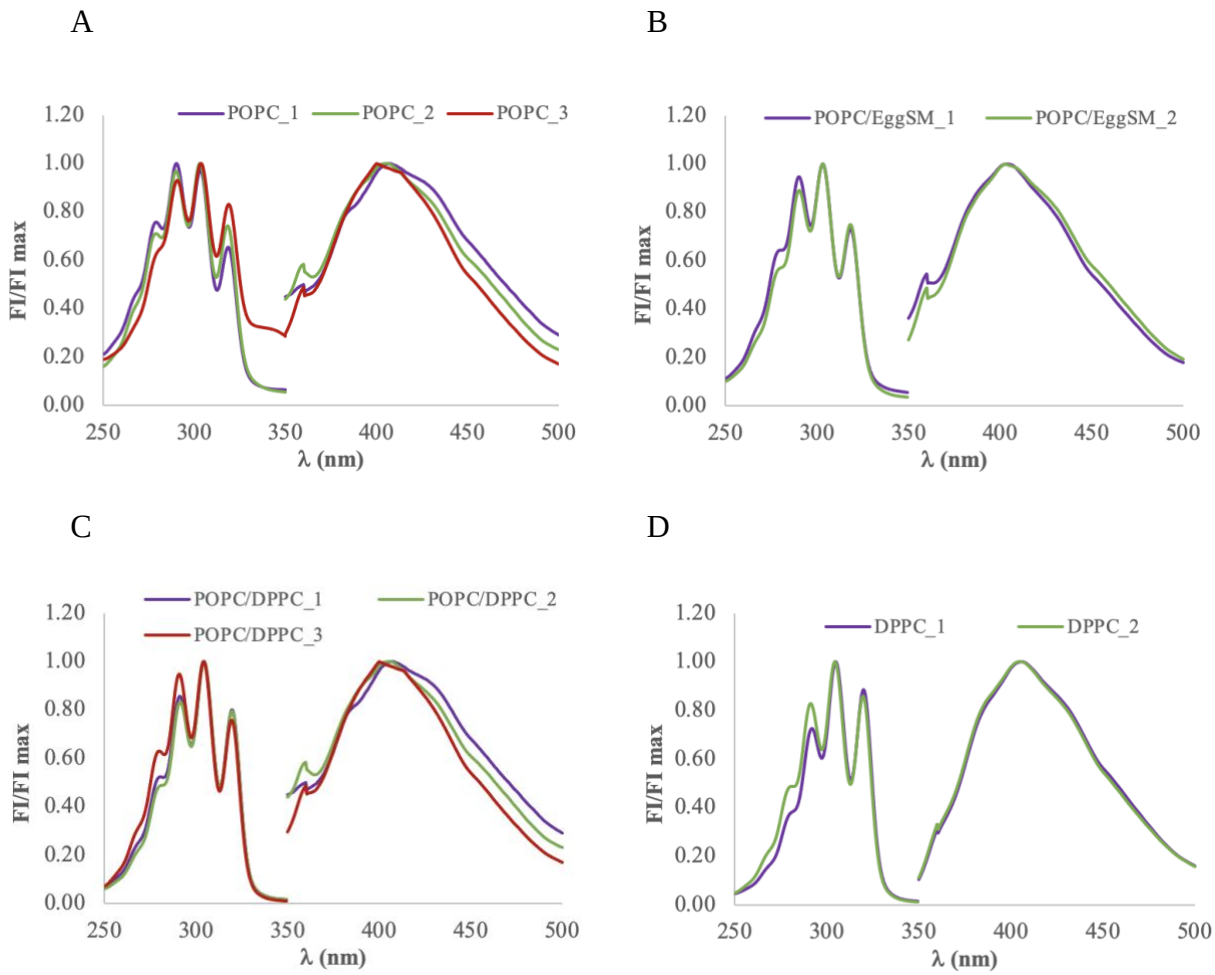

Figure 6. Effect of preparation method on the properties of various lipid mixtures. The normalized excitation and emission spectra of *t*-PnA were acquired using λex/λem 320/420 nm in (A) POPC, (B) POPC/EggSM, (C) POPC/DPPC, and (D) DPPC. The liposomes were prepared using the methods (purple) 1, (green) 2 and (red) 3 described in Table 1.1.

4.2 Fluorescence analysis of Nystatin in different lipidic mixtures

To better understand the interaction between nystatin and membranes of different lipid composition, the alterations in the photophysical properties of Nys were evaluated in the presence of POPC, POPC/EggSM (7:3), POPC/DPPC (1:1) and DPPC-containing vesicles. Previous studies have shown that the main factors controlling Nys's fluorescence spectra are Nys oligomeric state and packing properties of the membrane. (36)

4.2.1 Effect of lipid composition on Nys photophysical properties

Upon examination of the nystatin spectra across various lipid mixtures, notable similarities are observed between POPC and POPC/EggSM, while distinct alterations are present in mixtures containing DPPC. An increase in Nys fluorescence intensity accompanied by a blue-shift in its emission spectra is observed in the presence of DPPC. This is more pronounced in membranes containing pure DPPC, suggesting that the gel phase determines Nys photophysical behavior. This is further observed when comparing the ratios between the absorption peak ratios. An increase in the ratio between the peaks at shorter and longer wavelengths (FI 295/324nm) is observed in membranes containing DPPC. In the absence of DPPC, i.e. in POPC and POPC/EggSM no significant spectral shifts were observed (Figure 7), suggesting that changing the lipid composition of a fluid phase membrane do not significantly impact on Nys properties.

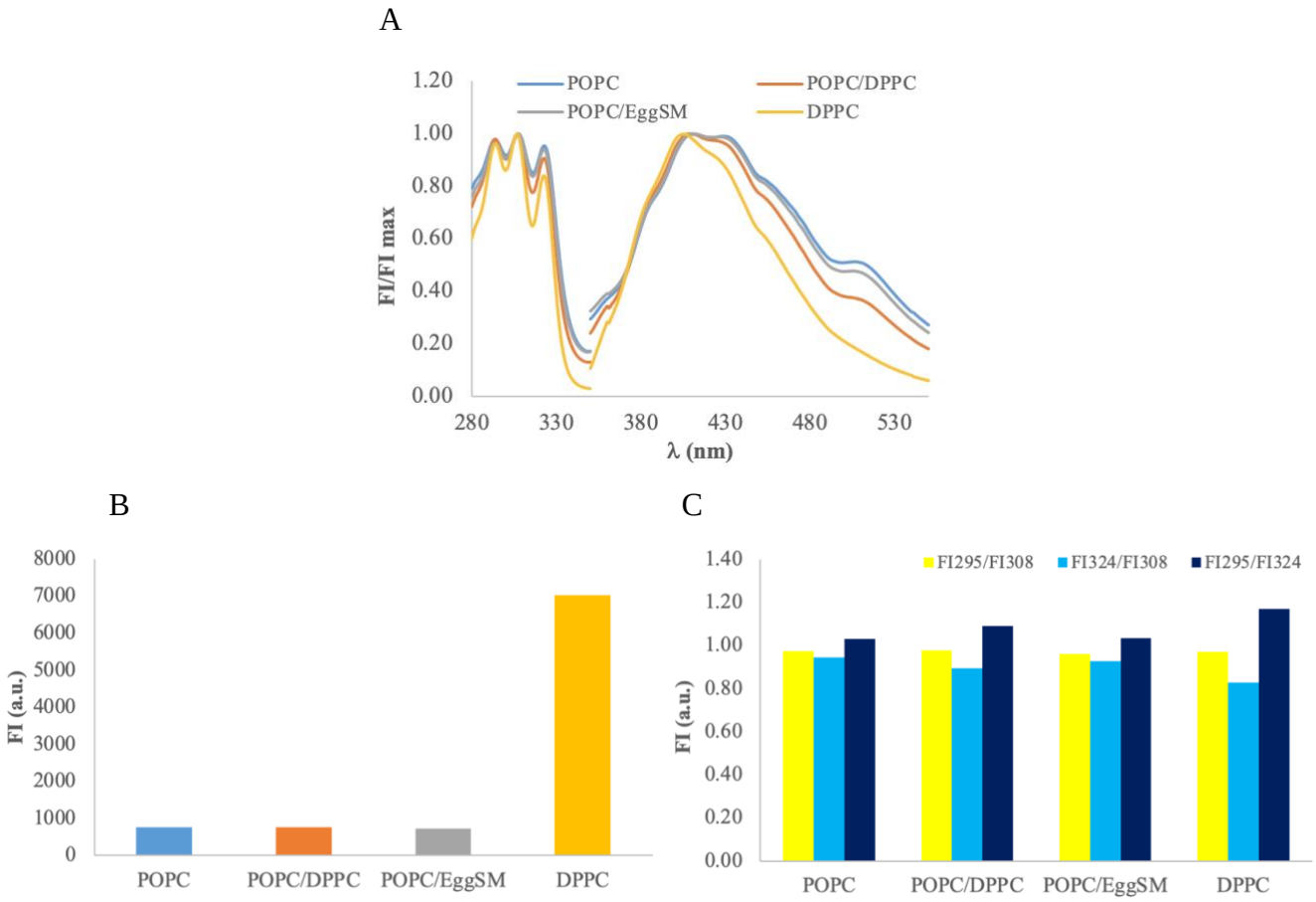

Figure 7. Variation of Nys' photophysical properties in the presence of membranes with different lipid compositions. (A) Normalized excitation and emission spectra of 15 µM Nys in POPC (blue), POPC/EggSM (grey), POPC/DPPC (orange), and DPPC (dark yellow). Spectra were acquired using λex/λem 303/404 nm. (B) Maximum fluorescence intensity taken from the emission spectra and (C) ratio between the fluorescence intensity at each peak of the excitation spectra in which yellow is FI295/FI308, light blue is FI324/FI308and dark blue is FI295/FI324.

4.2.2 Effect of Nys concentration on Nys-membrane interactions

To better address the effects of Nys, studies were performed using different lipid mixtures and Nys concentrations. Increasing the concentration of Nys caused a redshift in the maximum emission wavelength, which was more pronounced in fluid phase membranes. Significant differences in emission wavelengths were also observed among the lipid mixtures: an increase in the gel phase content shifted the maximum emission towards shorter wavelengths.

In addition, the results showed an increase in the fluorescence intensity with increasing Nys concentration. This variation was particularly strong in gel-phase DPPC membranes. Interestingly, a relationship between Nys concentration and absorption at

308 nm appeared in all lipid compositions except for DPPC membranes. Interestingly, an increase in anisotropy was observed for increasing concentrations of Nys, except in gel-phase DPPC membranes where the anisotropy decreased with Nys content. Nonetheless, Nys anisotropy values were higher in DPPC and decreased with increased membrane fluidity.

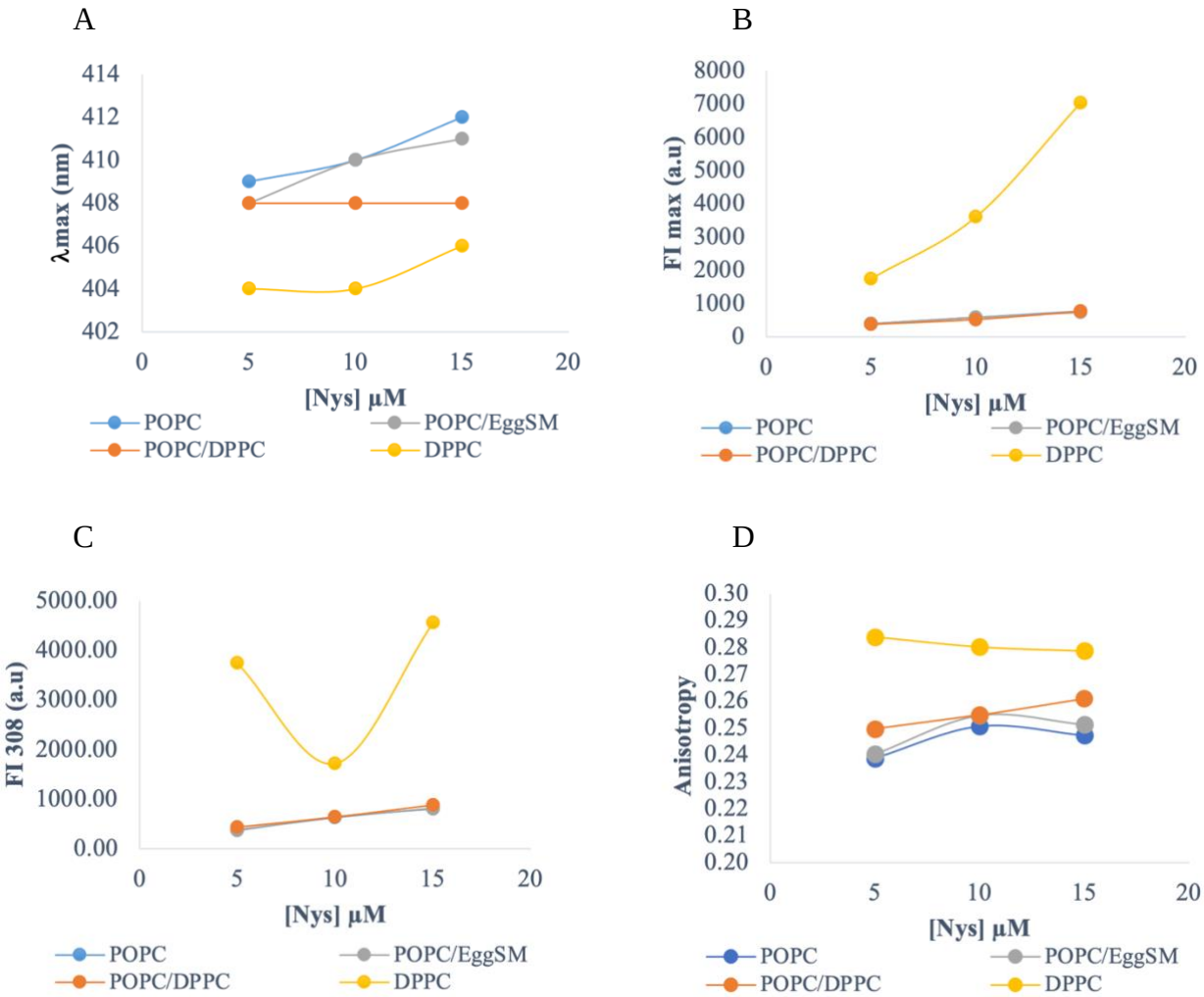

Figure 8. Analysis of Nys-membrane interactions with different Nys concentrations. Variation in (A) maximum emission wavelength, (B) maximum fluorescence intensity, (C) fluorescence intensity measured at 308 nm from the excitation spectra, and (D) steady-state fluorescence anisotropy of Nys at different concentrations in POPC (blue), POPC/EggSM (grey), POPC/DPPC (orange), and DPPC (dark yellow).

4.3 Influence of Nystatin on the Size Distribution of Liposomes

The liposomes analyzed in DLS were with POPC and POPC/DPPC. Several measurements were taken at different times after the addition of nystatin, with the 0-minute timepoint serving as a comparison for the different samples of Nys, since it does not contain the antifungal. A significant size heterogeneity was observed for both compositions, where several broad peaks, corresponding to populations with different size averages were observed (Figure 9). Upon adding Nys, a time-dependent shift in the peaks was observed, with increasingly clear separation between the different populations over time. The presence of larger sized-populations, suggests potential liposome aggregation over time.

A1 – POPC (0 min)

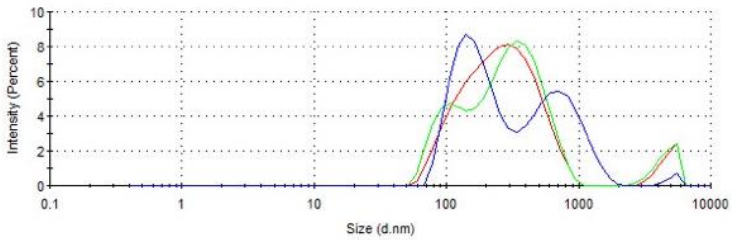

A2 – POPC (5 min)

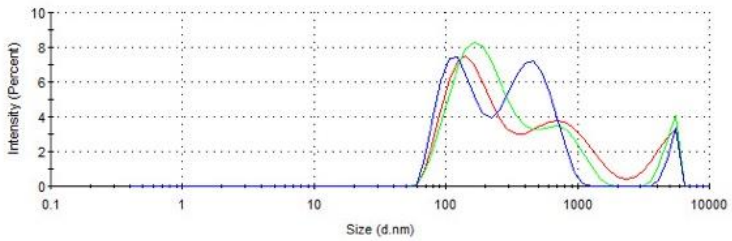

A3 – POPC (30 min)

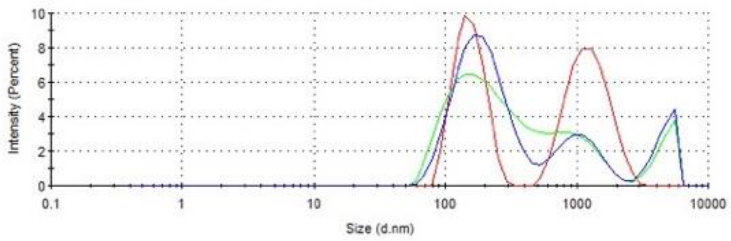

A4 – POPC (60 min)

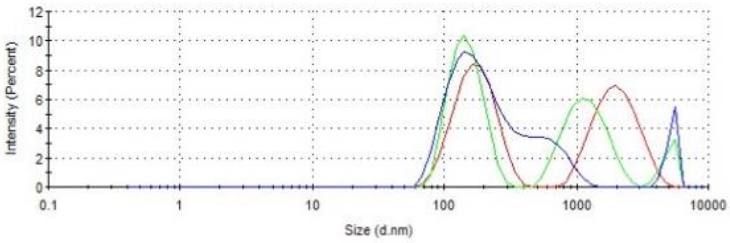

A5 – POPC (120 min)

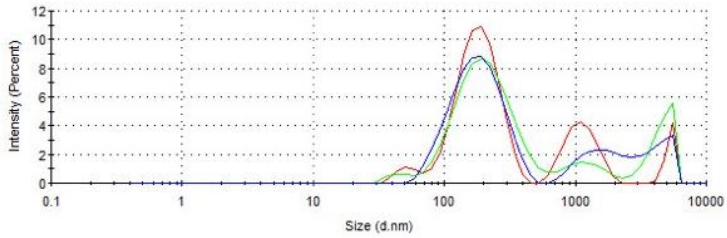

B1 – POPC/DPPC (0 min)

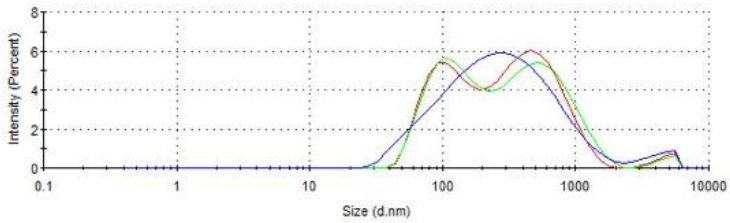

B2 – POPC/DPPC (5 min)

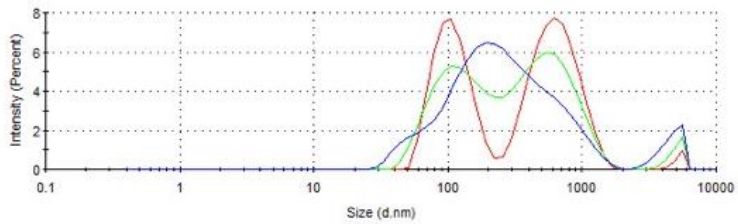

B3 – POPC /DPPC (30 min)

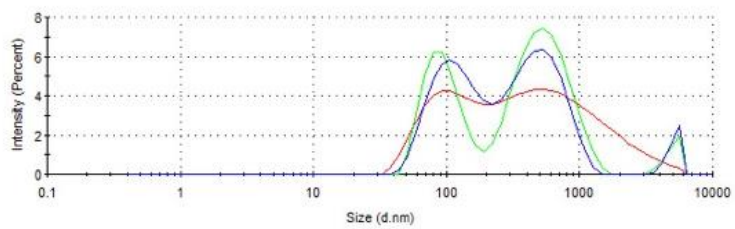

B4 – POPC/DPPC (60 min)

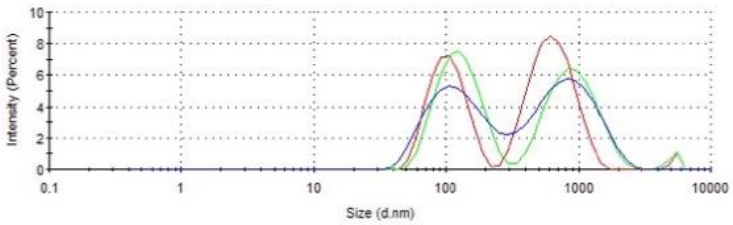

B5 – POPC/DPPC (120 min)

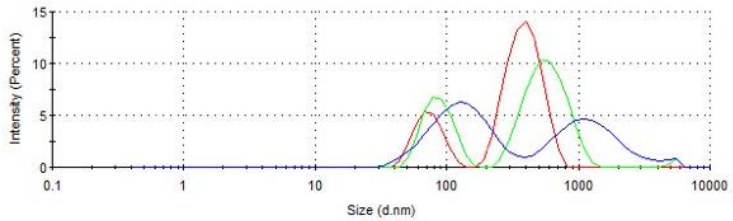

Figure 9. Influence of Nys on liposome size distribution. The intensity and size of each population were determined for (A) POPC and (B) POPC/DPPC after the addition of 15 µM Nys. Measurements were performed at five different time points: (A1, B1) 5 minutes, (A2 and B2) 10min, (A3 and B3) 30min, (A4 and B4) 60min and (A5 and B5) 120min. Each sample was measured 3 times: red the first, green the second and blue the third.

The PDI was notably high, ranging from 0.3 to 0.7 for all samples, which aligns with sample heterogeneity and broad particle size distribution (Figure 10 (B)). Although the presence of multiple populations limits the accuracy of the size measurements, an analysis was conducted to examine the variation in average particle size over time after the addition of Nys. Both POPC and POPC/DPPC mixtures showed an increase in average particle size over time, with POPC/DPPC generally maintaining a smaller average size compared to POPC (figure 10 (A)).

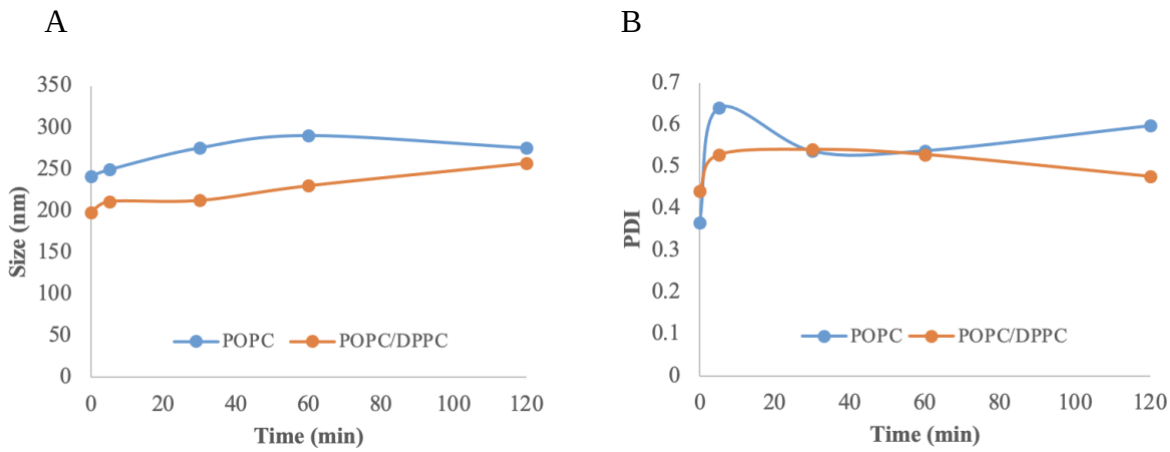

Figure 10. Nys effect on the average size and PDI of liposomes with different lipid composition. Variation of (A) the average size and the (B) PDI of POPC (blue) and POPC/DPPC (orange) liposomes before and, 5, 30, 60 and 120 minutes after addition of 15 µM Nys. Each sample was measured 3 times.

5 Discussion

Building on the assumption that nystatin exhibits a strong affinity for lipids, particularly in the gel phase, three different lipids were selected for this study. These included lipids with a T_m significantly above room temperature, such as DPPC and EggSM, as well as POPC, which has a low T_m and is widely characterized. The inclusion of POPC as the primary component of the fluid phase allows for a focused analysis of the gel phase interactions. (36)

The emission redshift observed with increasing nystatin concentration is notable in fluid membranes such as POPC and POPC/EggSM and in fluid-gel membranes such as POPC/DPPC, while DPPC, a gel-phase membrane, showed minimal shift, maintaining a consistent wavelength. In the emission spectra of DPPC, was also noticeable that the maximum wavelength occurred at shorter wavelengths, and so less energetic. This suggests that in gel phase Nys has less mobility, caused by the interaction with a gel-phase membrane or because it self-associates into a membrane-spanning pore, where the molecules are organized close together in a barrel-like structure. (5) Some studies suggest that this effect may result from pore formation, in which Nys molecules assemble in an oligomeric form that restricts molecular mobility. It was shown in activity studies that that addition of the antifungic to the vesicles without sterols lead to a complete dissipation of the gradient, indicating that Nys was able to permeabilize the membrane of the different lipid vesicles driving the formation of pores that lead to the total dissipation of the imposed K^+ gradient. (37) Although studies have shown improved pore formation characteristics in formulations containing sterols, they also indicate that sterols may not be strictly necessary, as Nys demonstrated a slow yet significant activity in sterol-free POPC liposomes under iso-osmotic conditions. (9) To further this research in our study and complete the hypotheses of possible pore formation in sterol-free membranes the partition coefficient of Nys should be determined to quantitatively evaluate the effects of Nys in the membrane and relate them with the lipid composition and properties of the vesicles. Also, activity studies are needed, this is, H^+/K^+ exchange assays across the membrane bilayer should be carried out to indirectly evaluate the effect of Nys on the potassium permeability of the lipid vesicles.

In our results, all mixtures showed an increase in maxima fluorescence intensity (FI_{max}) analyzed with the increase of Nys concentration, but there was a significant increase in the DPPC membrane, suggesting a strong increase in Nys quantum yield upon incorporation into DPPC-gel phase. As above mentioned, this can be caused by the stabilization of the tetraene moiety by the rigid gel phase, or due to the formation of Nys oligomers in the membrane. (37)

Through atomic force microscopy studies conducted on nystatin with supported membranes it was shown that addition of increasing nystatin concentration to POPC/DPPC lipid mixture of caused an increase in the gel phase area accompanied by a decrease in the thickness between gel and fluid phases (5). Interestingly, while these results suggest a higher fraction of the gel phase, they also suggest that alterations in the rigidity either of the fluid or of the gel phase might occur. In fact, a decrease in the thickness gap can be caused by a decrease in the height of the gel phase or an increase in the height of the fluid phase. This phenomenon could be potentially caused by an increased fluidity of the gel phase or decreased fluidity of the fluid phase. Interestingly, our results showing a concentration-dependent decrease in Nys anisotropy in DPPC membranes, suggest that this antifungal destabilizes the ordered packing of the DPPC-gel phase. On the other hand, the observed increase in Nys anisotropy in POPC/DPPC membranes aligns with the evidence from AFM showing expansion in the gel phase area upon addition of Nys. (5) In pure gel phase membranes, the extent of the gel phase should not change, and variations in Nys parameters likely reflect changes in the organization of the membrane. Accordingly, the decreased anisotropy coupled to a red-shift in the emission maximum in the presence of DPPC gel-phase membranes suggest a destabilization of the bilayer packing while the strong increase in the fluorescence intensity of the Nys points towards a stabilization of the tetraene, suggesting the formation of Nys oligomers. This hypothesis is supported by studies showing that Nys can form pores in DPPC membranes. (5)

In this study we further analyzed if the presence of EggSM in fluid membranes would significantly affect the photophysical properties of Nys. Compared to POPC no major differences were observed in Nys spectra and anisotropy, suggesting that Nys interaction with fluid phase membranes is not significantly affected by the type of lipid present in the fluid membrane. Nonetheless, previous studies have shown that in fluid EggSM-containing membranes Nys was still able to dissipate ca. 40% of the gradient

(5), which was accompanied by a slight increase in Nys lifetime, while in the absence of EggSM the ability of Nys to dissipate a potassium gradient and form long lived species is strongly decreased. (5) These results suggest that the fluid phase lipid composition also influences Nys-membrane interactions and further studies should be performed to better elucidate this question. Differences in the hydrogen bonding patterns due to the presence of a sphingoid backbone in SM, compared to the acyl chains in POPC, might facilitate Nys ability to partition into the membrane and form pores. (5)

In the present work, DLS studies were performed to address whether Nys pore formation would affect liposome integrity. Unfortunately, the liposomes exhibited significant variation in size and PDI values, making it challenging to establish a clear pattern for the effects of Nys addition. These studies should be repeated to allow for a more precise assessment of Nys's impact, and in the future, conducting these experiments alongside permeability assays could help determine if pore formation contributes to vesicle destabilization, potentially leading to aggregation and fusion. Additionally, microscopy analyses could enable direct observation of structural changes in the vesicles. Such phenomena may not be limited solely to the organization and phase properties noted in previous studies, like those observed through atomic force microscopy, but could also involve more drastic alterations in liposome structure, compromising their integrity. (5)

6 Conclusion

Nystatin, despite being an antifungal agent with considerable potential, does not fully achieve its therapeutic benefits due to challenges associated with systemic administration. To investigate hypotheses that may mitigate this limitation, the present study examined the interaction of nystatin with lipid membranes in both fluid and gel phases. The goal was to elucidate the differences in the interaction of the antifungal agent with distinct phases and lipids..

The results revealed significant variations particularly in membranes composed of DPPC, which behaved distinctly compared to other lipid combinations. The results obtained in this study suggest that nystatin interacts with sterol-free membranes and the mechanism is likely dependent on both lipid composition and membrane phase properties.

This research may serve as a valuable framework for future investigations involving other types of phospholipids or sphingolipids for liposome formulation, as well as more complex studies on nystatin behavior in fungal systems with the optimal liposome formulations studied. Ultimately, the aim is to develop potential formulations for drug delivery systems that optimize the therapeutic utility of this antifungal agent in the future.

References

1. Pound MW, Townsend ML, Dimondi V, Wilson D, Drew RH. Overview of treatment options for invasive fungal infections. Med Mycol. 2011 Mar 3;1–20.
2. Lyu X, Zhao C, Yan ZM, Hua H. Efficacy of nystatin for the treatment of oral candidiasis: A systematic review and meta-analysis. Drug Des Devel Ther. 2016;10.
3. Sousa F, Nascimento C, Ferreira D, Reis S, Costa P. Reviving the interest in the versatile drug nystatin: A multitude of strategies to increase its potential as an effective and safe antifungal agent. Vol. 199, Advanced Drug Delivery Reviews. Elsevier B.V.; 2023.
4. Zielinski J, Golik J, Pawlak J, Borowski E, Falkowski L. The structure of nystatin A3, a component of nystatin complex. J Antibiot (Tokyo). 1988 Sep;41(9):1289–91.
5. dos Santos AG, Marquês JT, Carreira AC, Castro IR, Viana AS, Mingeot-Leclercq MP, et al. The molecular mechanism of Nystatin action is dependent on the membrane biophysical properties and lipid composition. Physical Chemistry Chemical Physics. 2017;19(44):30078–88.
6. Bolard J. How do the polyene macrolide antibiotics affect the cellular membrane properties? Biochim Biophys Acta. 1986 Dec 22;864(3–4):257–304.
7. Silva L, Coutinho A, Fedorov A, Prieto M. Nystatin-induced lipid vesicles permeabilization is strongly dependent on sterol structure. Biochim Biophys Acta Biomembr. 2006;1758(4):452–9.
8. Aresta-Branco F, Cordeiro AM, Marinho HS, Cyrne L, Antunes F, de Almeida RFM. Gel domains in the plasma membrane of Saccharomyces cerevisiae: highly ordered, ergosterol-free, and sphingolipid-enriched lipid rafts. J Biol Chem. 2011 Feb 18;286(7):5043–54.
9. Coutinho A, Silva L, Fedorov A, Prieto M. Cholesterol and ergosterol influence nystatin surface aggregation: relation to pore formation. Biophys J. 2004 Nov;87(5):3264–76.

10. Pedro F, Santos C, Orientada T, Rodrigo D, De Almeida FM, Presidente J:, et al. Sphingolipid domains in the plasma membrane of fungal cells Interplay with membrane proteins and antifungal resistance Doutoramento em Bioquímica Especialidade: Biofísica Molecular.

11. Hein R, Uzundal CB, Hennig A. Simple and rapid quantification of phospholipids for supramolecular membrane transport assays. Org Biomol Chem. 2016;14(7):2182–5.

12. Immordino ML, Dosio F, Cattel L. Stealth liposomes: review of the basic science, rationale, and clinical applications, existing and potential. Int J Nanomedicine. 2006;1(3):297–315.

13. Grit M, Crommelin DJA. Chemical stability of liposomes: implications for their physical stability. Chem Phys Lipids. 1993 Sep;64(1–3):3–18.

14. Akbarzadeh A, Rezaei-Sadabady R, Davaran S, Joo SW, Zarghami N, Hanifehpour Y, et al. Liposome: classification, preparation, and applications. Nanoscale Res Lett. 2013 Feb 22;8(1):102.

15. Wagner A, Vorauer-Uhl K. Liposome technology for industrial purposes. J Drug Deliv. 2011;2011:591325.

16. Zou Y, Lee HY, Seo YC, Ahn J. Enhanced antimicrobial activity of nisin-loaded liposomal nanoparticles against foodborne pathogens. J Food Sci. 2012 Mar;77(3):M165-70.

17. Paszko E, Senge MO. Immunoliposomes. Curr Med Chem. 2012;19(31):5239–77.

18. Francesca Fedeli, Chiarma Profssa Annalisa Santucci Correlatore Chiarmo Rodrigo de Almeida R. DIPARTIMENTO DI BIOTECNOLOGIE, CHIMICA E FARMACIA CORSO DI LAUREA MAGISTRALE IN CHIMICA E TECNOLOGIA FARMACEUTICHE Understanding the action of Nystatin: studies with liposomes as membrane model and drug delivery systems. 2018.

19. Hesketh R. Triplet Deciphers Genomes: Molecular Cell Biology (4th Edition). J Cell Sci. 2000 Sep 1;113(17):2925–6.

20. Ramos-Martín F, D'Amelio N. Biomembrane lipids: When physics and chemistry join to shape biological activity. Biochimie. 2022 Dec;203:118–38.

21. Jing Y, Trefna H, Persson M, Kasemo B, Svedhem S. Formation of supported lipid bilayers on silica: relation to lipid phase transition temperature and liposome size. Soft Matter. 2014;10(1):187–95.

22. Zhang Z, Hao C, Qu H, Sun R. Studied on the dynamic adsorption process of Lycium barbarum polysaccharide in the POPC/DPPC monolayers. Colloids Surf B Biointerfaces. 2019 Jun;178:38–43.

23. Blesso C. Egg Phospholipids and Cardiovascular Health. Nutrients. 2015 Apr 13;7(4):2731–47.

24. Arsov Z, González-Ramírez EJ, Goñi FM, Tristram-Nagle S, Nagle JF. Phase behavior of palmitoyl and egg sphingomyelin. Chem Phys Lipids. 2018 Jul;213:102–10.

25. Lakowick, JR. Principles of Fluorescence Spectroscopy. Scholars Portal; 1999.

26. Naresh K. National Level Workshop on Spectroscopic Techniques in Structural Elucidation Journal of Chemical and Pharmaceutical Sciences Applications of Fluorescence Spectroscopy. Available from: www.jchps.com

27. Castanho M, Prieto M, Ulises Acuña A. The transverse location of the fluorescent probe trans-parinaric acid in lipid bilayers. Biochimica et Biophysica Acta (BBA) - Biomembranes. 1996 Mar;1279(2):164–8.

28. Coutinho A, Prieto M. Self-association of the polyene antibiotic nystatin in dipalmitoylphosphatidylcholine vesicles: a time-resolved fluorescence study. Biophys J. 1995 Dec;69(6):2541–57.

29. Sklar LA, Hudson BS, Petersen M, Diamond J. Conjugated polyene fatty acids as fluorescent probes: spectroscopic characterization. Biochemistry. 1977 Mar 8;16(5):813–9.

30. Castanho MA, Coutinho A, Prieto MJ. Absorption and fluorescence spectra of polyene antibiotics in the presence of cholesterol. J Biol Chem. 1992 Jan 5;267(1):204–9.

31. Nickel C, Angelstorf J, Bienert R, Burkart C, Gabsch S, Giebner S, et al. Dynamic light-scattering measurement comparability of nanomaterial suspensions. Journal of Nanoparticle Research. 2014 Feb 25;16(2):2260.

32. Bhattacharjee S. DLS and zeta potential – What they are and what they are not? Journal of Controlled Release. 2016 Aug;235:337–51.

33. Farkas N, Kramar JA. Dynamic Light Scattering Distributions by Any Means. J Nanopart Res. 2021 May;23(5).

34. Stetefeld J, McKenna SA, Patel TR. Dynamic light scattering: a practical guide and applications in biomedical sciences. Biophys Rev. 2016 Dec;8(4):409–27.

35. Lorber B, Fischer F, Bailly M, Roy H, Kern D. Protein analysis by dynamic light scattering: methods and techniques for students. Biochem Mol Biol Educ. 2012;40(6):372–82.

36. Silva L, Coutinho A, Fedorov A, Prieto M. Nystatin-induced lipid vesicles permeabilization is strongly dependent on sterol structure. Biochimica et Biophysica Acta (BBA) - Biomembranes. 2006 Apr;1758(4):452–9.

37. Silva L, Coutinho A, Fedorov A, Prieto M. Competitive Binding of Cholesterol and Ergosterol to the Polyene Antibiotic Nystatin. A Fluorescence Study. Biophys J. 2006 May;90(10):3625–31.